

# Deep Feature Detection Approach for COVID-19 Classification based on X-ray Images

Ayman Noor<sup>1</sup>, Priyadarshini Pattanaik<sup>2</sup>, Mohammed Zubair Khan<sup>3</sup>, Waseem Alromema<sup>4</sup>, Talal H. Noor<sup>5</sup>

College of Computer Science and Engineering, Taibah University, Madinah, Saudi Arabia<sup>1</sup>

Department of Computer Science & Engineering-School of Engineering and Technology (SET), Sharda University<sup>2</sup>

Department of Computer Science and Information, Taibah University, Medina 42353, Saudi Arabia<sup>3,4</sup>

College of Computer Science and Engineering, Taibah University, Yanbu, Madinah, Saudi Arabia<sup>5</sup>

**Abstract**—The novel human Corona disease (COVID-19) is a pulmonary sickness brought on by an extraordinarily outrageous respiratory condition crown 2. (SARS -CoV-2). Chest radiography imaging has a significant role in the screening, early diagnosis, and follow-up of the suspected individuals due to the effects of COVID-19 on pneumonic-sensitive tissue. It also has a severe impact on the economy as a whole. If positive patients are identified early, the spread of the pandemic illness can be slowed. To determine whether people are at risk for illnesses, a COVID-19 infection prediction is critical. This paper categorizes chest CT samples of COVID-19 affected patients. The two-stage proposed deep learning technique produces spatial function from images, so it is a very expeditious manner for image category hassle. Extensive experiments are drawn by considering the benchmark chest-Computed Tomography (chest-CT) image datasets. Comparative evaluation reveals that our proposed method outperforms amongst other 20 different existing pre-trained models. The test outcomes constitute that our proposed model achieved the best rating of 97.6%, 0.964, 0.964, and 0.982 concerning the accuracy, precision, recall, specificity, and F1-score, respectively.

**Keywords**—COVID-19; coronavirus; deep learning; classification; chest X-ray images; DenseNet-121; XG-Boost classifier; EfficientNet-B0

## I. INTRODUCTION

COVID-19 has become a global health emergency of concern since it was first identified in December 2019. It is generating unheard-of societal and economic devastation. According to the WHO report, by March 29, 2021, there were 126,890,643 afflicted people worldwide, 2,778,619 of whom passed away. There is a severe scarcity of medical resources as a result of the global COVID-19 pandemic, which has put tremendous strain on healthcare institutions. Coronavirus pneumonia has been known as COVID-19 since its discovery, and it is both exceedingly contagious and harmful [1][2]. Pneumonia could arise if the signs get worse. Major health problems and the failure of numerous organs may ensue from this. Additionally, the patient is at risk of getting severe pneumonia. Medical practitioners, governments, organizations, and nations from all over the world face significant difficulty in trying to diagnose people with COVID-19 as soon as possible. Even though immunological testing is generally accessible, COVID-19 is frequently identified via RT-PCR, or Real-Time Polymerase Chain reaction (rt Chain Reaction). Images of patients' lungs can be used to detect the harmful effects of

COVID-19 and ensure prompt treatment rather than depending on RT-PCR, which has a low susceptibility (60-70%) and is also a time-consuming procedure. When providing care for patients who have COVID-19, it is imperative to closely observe how a patient's status evolves. When used in conjunction with additional diagnostic testing, medical imaging techniques like Computed Tomography (CT) and chest X-rays can be used to monitor the patient's progress and confirm the diagnosis of COVID-19 pneumonia. These images demonstrate the rapid onset of ground-glass opacities following the onset of COVID-19 symptoms.

Artificial Intelligence (AI) is broad term for several methods intended to simulate human thought and behavior (AI). The development of methods that enable powerful computers to recognize complex patterns and connections in empirical data is the focus of a branch of artificial intelligence known as "Machine Learning" (ML) [4]. To acquire greater power and flexibility, Deep Learning (DL) draws inspiration from biological neural networks. In contrast to typical ML approaches [8], which are restricted in their ability to handle complicated problems like the classification of medical images, DL is inspired by biological neural networks to achieve better power and flexibility.

A significant collection of images that have been tagged is necessary for a DL-based detection or classification system to function well. Deep Feature Detection (DFD) and Transfer Learning (TL) are the best alternatives to using a limited sample size of images when a large sample size is not practical TL. Teaching a language involves using strategies that have already been learned to get around unexpected barriers (TL). TL is a method that can be used to build a new machine learning model, not a particular category of algorithms. The model will be able to apply the knowledge and skills it has acquired from prior training to novel circumstances [3][4][5]. The data must be organized by file type, just like in the previous step. Another application for TL is the extraction of deep feature data. Instead of manually changing the CNN's activation layers, feature vectors can be extracted using pre-trained CNN models. Installations of lower-level layers activate deeper layers that contain higher-level components crucial for detecting visuals [6].

The article addresses the above gaps including limited training data, class imbalance, interpretability challenges, robustness to variations, and transferability issues across

populations. To address these gaps, there is a need for more large datasets, improved model interpretability, better handling of class imbalance, enhanced robustness to image variations, and increased transferability to different populations. Addressing these gaps is vital for enhancing the accuracy and reliability of deep learning models in COVID-19 classification using X-ray images.

To distinguish between patients with COVID-19 infection and healthy people, this work presents a DFD-based method that makes use of XG-Boost [6][7]. The whole article is briefly reviewed in Section II, and the database and different methodologies are explained in Section III. In Section IV, the proposed work is introduced and the whole experimental work with results is explained in Section V. Section VI discusses the findings and Section VII concludes the research work with future outlook.

## II. REVIEW WORK

Recently, researchers observed imaging patterns on chest CT to detect COVID-19. Lunagariya et al. [24] used TL to train Squeeze Net, DenseNet-121, and ResNet18 to distinguish between Covid-19-infected and non-infected individuals using CXR photos and were successful in identifying COVID-19. Gravitational search optimization-DenseNet121-COVID-19 was proposed by Khan et al. [19] suggested CoroNet, a deep CNN built on the Xception paradigm, as a way to distinguish Covid-19 from CXRs. The COVID-19 and Multiclass Xception models are used to categorize pneumonia in this study. H. Panwar et al. [20] introduce a novel method that combines deep learning techniques with gradient-weighted Class Activation Mapping (grad-CAM) for the swift identification of COVID-19 cases using chest X-ray and CT-scan images. The authors propose a color visualization technique to enhance the interpretability of the deep learning model's findings. The article showcases the experimental results, highlighting the potential of their approach in quickly and accurately detecting COVID-19 cases based on medical imaging data. Luz et al. [21], the authors discuss their efforts to develop a deep-learning model that can accurately and efficiently detect COVID-19 patterns in X-ray images. The authors detail their approach, and techniques employed, and present the outcomes of their experiments conducted to train and assess the model's performance. The article emphasizes the potential of deep learning methods in aiding the detection and diagnosis of COVID-19 through X-ray imaging technology. J. Zhang et al. [22] used 100 CXRs from COVID-19 cases and pre-trained weights from the ImageNet database to build their ResNet-based model. With an f-score of 0.72, their top model could distinguish between CAP and COVID-19 infection. Eduardo Luz et al. [23] demonstrated a DFE-based hierarchical categorization technique using EfficientNet models [11][12]. Classifiers are located between the tree's nodes, whereas target categories are located at the tree's leaves. At the root node, one classifier was used to separate the Normal and Pneumonia patients, while another classifier was used at a higher level to separate the Pneumonia patients only.

## III. DATABASE AND METHOD ANALYSIS

The COVID-19, Pneumonia, and Healthy Chest X-ray PA Dataset [9][10] is being used in this study, and it was available

in April 2021. This data set contains 4575 images divided into three groups of 1525 images each. The images were obtained from a variety of web resources by the dataset's creator. The dataset contains chest X-ray Poster Anterior (PA) images and is divided into three categories (covid, pneumonia, and normal). GitHub, Radiopaedia, The Cancer Imaging Archive (TCIA), and the Italian Society of Radiology were used to collect 613 X-ray images of COVID-19 cases (SIRM). Rather than having the data independently enhanced, a dataset with 912 already-augmented images was obtained from Mendeley. 1525 images were obtained from the Kaggle repository and the NIH dataset. To validate a proposed technique, the experimental dataset is divided into two parts: training and testing. The remaining 30% of the images are used to test the effectiveness of the proposed technique, while the training set consists of 70% randomly selected images (i.e., 3202). (i.e., 1373). The assessment measure for each pre-trained model is created by combining ten cycles of a training-testing assessment in which different sets of randomly selected images are used for both the supplied model's training and testing.

The training set comprised 70% of the total dataset, while the test set comprised 30%. The dataset was further divided into three sections: learning, validation, and testing. To employ the transfer learning strategy, following are used:

**EfficientNet-B0:** Unlike custom, the EfficientNet-B0 [4][5][6] scaling method uses a set of predetermined scaling coefficients to gradually increase the network's resolution, depth, and width. EfficientNet-B0[4][5] scales the network's resolution, depth, and width using a compound coefficient. Compound scaling [6][9][11] was developed based on the idea that a larger input image requires more levels and channels in the networks to expand the available field and capture fine details on the larger image.

**DenseNet-121:** As a CNN's layers increase, the "vanishing gradient" problem becomes more common. As an alternative to using it, DenseNets-121[6][7] modifies the traditional CNN architecture and reduces the connections between the various layers. The name "Densely Connected Convolutional Network" is appropriate because each layer in the network is densely connected.

**Tune the XG-Boost Classifier [7]:** To accurately predict the outcome, the XG-Boost Classifier's parameters must be tweaked. The procedure for tuning is fully described in XG-Boost Classifier Tuning Algorithm 2, the maximum depth (MD), number of estimators (classification trees), and learning rate (LR) of each classification tree are XG-Boost classifier tuning parameters.

## IV. PROPOSED TECHNIQUE

Fig. 1 shows the proposed architecture. A two-step process is used to retrieve the X-ray image characteristics. In the first stage, a pre-trained model is used to extract features from a collection of all X-ray images [13]-[18]. After the features have been collected, they are ranked using the Recursive Feature Elimination method. Finally, it is decided to keep only the top-ranked characteristics. The following describes the two-stage feature extraction process using Algorithm 1 (Deep Feature Detection).

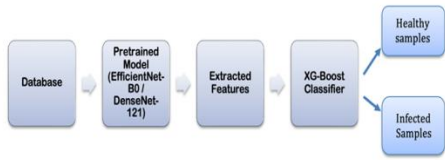


Fig. 1. Proposed two-stage deep feature detection technique.

The algorithm "Deep Feature Detection" is designed to extract deep features from a set of images using a pre-trained model. It takes as input a pre-trained model (M), a set of N images (I1, I2, ..., IN), and the desired size for the resized images (K\*K). The procedure involves removing non-convolutional layers from the pre-trained model to create a modified model (MR). An empty array called DF is initialized to store the extracted deep features. For each image in the set, the algorithm resizes it to the desired size and passes it through the modified model to obtain the features. These features are then flattened and added to the DF array. The algorithm also includes a step for ranking the features based on an unspecified criterion. Finally, the algorithm selects the features with a rank value of 1 and stores them in the selected features array. The output of the algorithm is a 2D array representing the selected deep features (DF).

**Algorithm 1:** Deep Feature Detection

Input: Pretrained Model (i.e. M), Set of 'N' Images I1 .. IN, Required Image Size (i.e., K\*K) Output: A 2D array of chosen deep features is produced (i.e., DF)

```

Procedure:
MR ← Remove_Non_Conv_Layers (M)
DF = []
for i=1 to N do
  Resize image Ii to size (K*K) features ← MR (Ii)
  features ← Flatten (features) DF.append (features)
feature_rank ← FeatureRanking (DF) selected_features = DF[feature_rank==1]
    
```

**Algorithm 2:** Tune XG-Boost Classifier

Input: 2D array of class labels and selected features, or deep features, Output: Best Parameters for Tuning the XGBoost Model

```

Procedure:
Acc_array = []
for max_depth = 3 to 5 do
  for learning_rate = 0.1 to 0.5 (step size 0.2) do
    for n_estimator = 300 to 800 (step size 50) do:
      accuracy ← K_Fold_XGBoostModelEvaluation (Folds=10, max_depth, learning_rate, n_estimators)
    acc_array [max_depth, learning_rate, n_estimators] ← Accuracy
  Select combinations of Parameters from acc_array which gives the highest accuracy.
    
```

V. EXPERIMENTAL RESULTS

The dataset [9], which was released in April 2021, is used for testing. This data set includes 4575 photos divided into

three groups of 1525 images each. These images as shown in Fig. 2 were obtained by the dataset's creator from a variety of web resources.

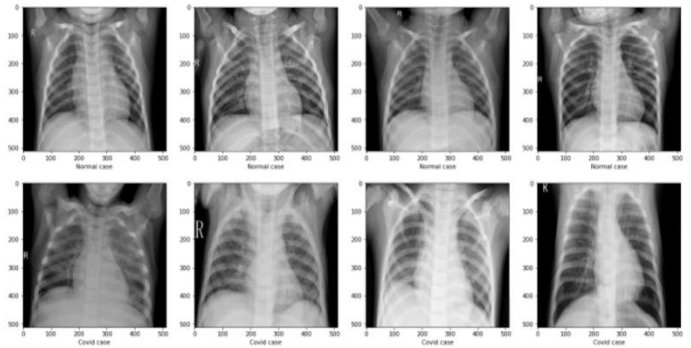


Fig. 2. Healthy and infected input dataset.

Using 10-fold cross-validation, the prediction accuracy of suggested experiments is investigated. The prediction accuracy of the XG-Boost Classifier, when trained using deep features detected using the DenseNet-121 model, is shown in Fig. 3, Table I, Table II, and Table III for various configurations of the Depth of the Tree, Learning Rate, and Number of Estimators variables. The model's classification accuracy is highest when trained with the values 0.3, 350, and 5 for the LR, MD, and classification trees, respectively. While, the prediction accuracy of the XG-Boost Classifier, when trained using deep features detected using the EfficientNetB0 model, is shown in Fig. 4 for various configurations of the Depth of the Tree, Learning Rate, and Number of Estimators variables. The model's classification accuracy is highest when trained with the values 0.3, 350, and 5 for the LR, MD, and classification trees, respectively.

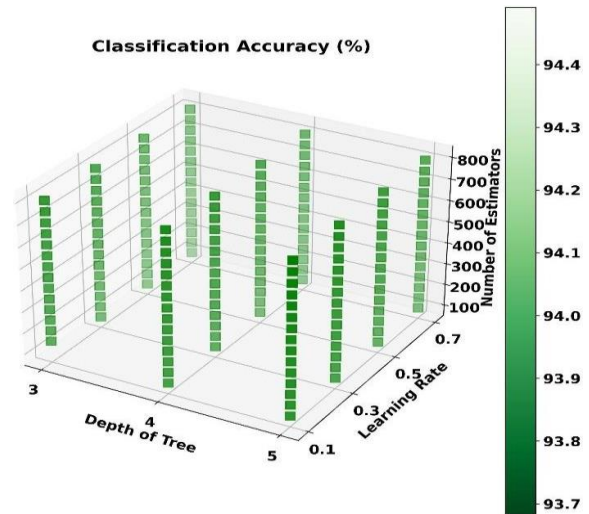


Fig. 3. XGBoost classifier's prediction accuracy for different tree depths, learning rates, and estimator counts when the classifier is trained using deep features from the DenseNet-121 model.

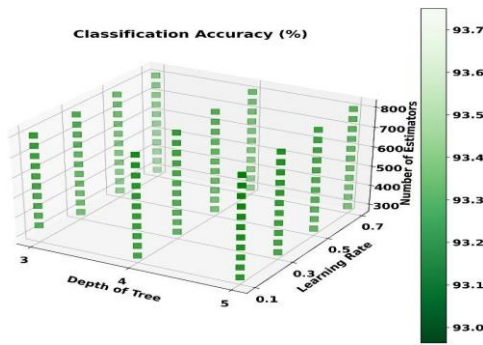


Fig. 4. XGBoost classifier's prediction accuracy for different tree depths, learning rates, and estimator counts when the classifier is trained using deep features taken from the EfficientNet-B0 model.

A. Model Name: DenseNet121 XG-Boost Balance Tune Results 128

Results-1:

Maximum depth is 3,

The learning rate is 0.1, 0.3, 0.5, and 0.7

Estimators range from 100 to 800

Accuracy Obtained: 0.94468524

TABLE I. ACCURACY OF DENSENET-121 WITH XG-BOOST CLASSIFIER, DEPTH 3 IN AN ESTIMATOR RANGE FROM 100 TO 800

Estimator	MD -3, LR. -0.1	MD -3, LR. -0.3	MD -3, LR. -0.5	MD -3, LR. -0.7
100	0.93025599	0.93769063	0.93921999	0.93987358
150	0.93746847	0.93878569	0.94053004	0.94271443
200	0.93877996	0.93922429	0.94183867	0.9422744
250	0.93987215	0.94163083	0.94249656	0.9422787
300	0.94205796	0.94096864	0.94337375	0.94249799
350	0.9416208	0.94074934	0.94424665	0.94271443
400	0.94249369	0.94075221	0.94424808	0.94249513
450	0.94227583	0.94053148	<b>0.94468524</b>	0.94271443
500	0.94293086	0.94096864	0.94424951	0.94205796
550	0.94315302	0.94140437	0.94403021	0.94205796
600	0.9422744	0.9411865	0.94381235	0.94205796
650	0.94315016	0.94096577	0.94403021	0.94227726
700	0.94292799	0.94074791	0.94403021	0.94271443
750	0.94271013	0.94074791	0.94402878	0.94293372
800	0.94292942	0.94074791	0.94424808	0.94249656

Results-2:

Maximum depth: 4,

Learning Rate: 0.1, 0.3,0.5,0.7

No of Estimators: from 100 to 800

Accuracy Achieved: 0.94489594

TABLE II. ACCURACY OF DENSENET-121 WITH XG-BOOST CLASSIFIER, DEPTH 4 IN AN ESTIMATOR RANGE FROM 100 TO 800

Estimator	MD -3, lr. -0.1	MD -3, lr. -0.3	MD -3, lr. -0.5	MD -3, lr. -0.7
100	0.93680914	0.94359305	0.94052718	0.94227583
150	0.94009431	0.94381092	0.94074647	0.94271299
200	0.94118364	0.94402878	0.9411822	0.94227583
250	0.9416208	0.94358875	0.94205796	0.94205653
300	0.94358445	0.94337232	0.94249656	0.94249369
350	0.94402305	0.94359019	0.9420594	0.9422744
400	0.94446164	0.94293516	0.9416208	0.94271299
450	0.94467951	0.94315446	0.9416208	0.94205653
500	0.94467808	0.94315446	0.9420594	0.94227583
550	0.94423948	0.94337232	0.94249656	0.94227583
600	0.94467664	0.94337089	0.94227726	0.94227726
650	0.94467664	0.94359019	0.94249656	0.94205796
700	0.94467664	0.94402735	0.94271586	0.9416208
750	<b>0.94489594</b>	0.94358875	0.94249656	0.94271443
800	0.94467808	0.94336945	0.94271586	0.94293229

Result-3:

Maximum Depth: 5,

Learning Rate: 0.1, 0.3,0.5,0.7

No of Estimators from 100 to 800

Accuracy Achieved: 0.94491027

TABLE III. ACCURACY OF DENSENET-121 WITH XG-BOOST CLASSIFIER, DEPTH 5 IN AN ESTIMATOR RANGE FROM 100 TO 800

Estimator	MD -3, LR. -0.1	MD -3, LR. -0.3	MD -3, LR. -0.5	MD -3, LR. -0.7
100	0.93681487	0.94206656	0.9422744	0.93987501
150	0.93922142	0.94425381	0.94205653	0.94009145
200	0.9416294	0.94381808	0.94380662	0.94009145
250	0.94184727	0.94469098	0.94424665	0.94074791
300	0.94206656	0.94425238	0.94402735	0.94074934
350	0.94272016	<b>0.94491027</b>	0.94424521	0.94052718
400	0.94337662	0.94425525	0.94468381	0.94030931
450	0.94403165	0.94403308	0.94402591	0.94031218
500	0.94468954	0.94359449	0.94402591	0.94030931
550	0.94424951	0.94403021	0.94358732	0.94053004
600	0.94468668	0.94424951	0.94380518	0.94074791
650	0.94446738	0.94403165	0.94380518	0.94052861
700	0.94403021	0.94424951	0.94380518	0.94053004
750	0.94446881	0.94490597	0.94380518	0.94009431
800	0.94403165	0.94490454	0.94402305	0.94031361

B. Model Name: EfficientNetB0\_XG-Boost\_Balance\_Tune\_Results\_128

Results-1:

Maximum depth: 3,

Learning Rate-0.1, 0.3,0.5, 0.7

No of Estimators from 300 to 800

Accuracy Achieved: 0.93750143

TABLE IV. ACCURACY OF EFFICIENTNETB0 WITH XG-BOOST CLASSIFIER, DEPTH 3 IN AN ESTIMATOR RANGE FROM 100 TO 800

Estimator	MD -3 , lr. -0.1	MD -3 , lr. -0.3	MD -3 , lr. -0.5	MD -3 , lr. -0.7
300	0.92963823	0.9331384	0.93531705	0.9329191
350	0.9296368	0.93313697	0.93531705	0.93248051
400	0.93029039	0.93226551	0.93640924	0.93313697
450	0.93094399	0.93226264	0.93640781	0.93226408
500	0.93138258	0.93204478	0.93662711	0.93248194
550	0.93203618	0.93226264	0.93706427	0.93248051
600	0.93203904	0.93269837	0.93706427	0.93269694
650	0.93247621	0.9333534	0.93706427	0.93247764
700	0.93269551	0.9333534	0.9375	0.93247907
750	0.93269551	0.93335197	0.93706427	0.93225978
800	0.93313267	0.93356983	<b>0.93750143</b>	0.93225978

Table IV showcases the performance of the EfficientNetB0 model combined with an XG-Boost classifier of depth 3 and an estimator range from 100 to 800, achieving an accuracy of 0.93750143.

Result-2:

Maximum depth: 4,

Learning Rate: 0.1, 0.3,0.5,0.7

No of Estimators from 300 to 800

Accuracy Achieved: 0.933357

TABLE V. ACCURACY OF EFFICIENTNETB0 WITH XG-BOOST CLASSIFIER, DEPTH 4 IN AN ESTIMATOR RANGE FROM 100 TO 800

Estimator	MD -3 , lr. -0.1	MD -3 , LR. -0.3	MD -3 , LR. -0.5	MD -3 , LR. -0.7
300	0.93095259	0.93161048	0.93270124	0.93116902
350	0.93160905	0.93182691	0.93292054	0.93160618
400	0.93138975	0.93182835	0.93292054	0.93160618
450	0.93160761	0.93204764	0.93270267	0.93138832
500	0.93204191	0.93204621	0.93204621	0.93138975
550	0.93225978	0.93270411	0.93182835	0.93138832
600	0.93269837	0.93313984	0.93204621	0.93138832
650	0.93291624	0.93313984	0.93204764	0.93138832
700	0.93291767	0.93313984	0.93161191	0.93138832
750	0.93291624	<b>0.9333577</b>	0.93161048	0.93138832
800	0.93291624	0.93313984	0.93204908	0.93138832

Results-3:

Maximum depth: 5,

Learning Rate: 0.1, 0.3,0.5,0.7

No of Estimators from 300 to 800

Accuracy Achieved: 0.93314557

TABLE VI. ACCURACY OF EFFICIENTNETB0 WITH XG-BOOST CLASSIFIER, DEPTH 5 IN AN ESTIMATOR RANGE FROM 100 TO 800

Estimator	MD -3 , LR. -0.1	MD -3 , LR. -0.3	MD -3 , LR. -0.5	MD -3 , LR. -0.7
300	0.93007539	0.93095545	0.93160618	0.93205194
350	0.92985609	0.93117475	0.93117045	0.93248911
400	0.93029326	0.93139405	0.93117045	0.93292627
450	0.93051542	0.93183121	0.93117045	<b>0.93314557</b>
500	0.93160475	0.93204908	0.93095115	0.93292627
550	0.93116902	0.93204908	0.93160475	0.93270841

600	0.93138975	0.93204908	0.93160475	0.93249054
650	0.93138832	0.93182978	0.93160475	0.93205481
700	0.93138975	0.93161048	0.93182261	0.93249054
750	0.93160905	0.93161048	0.93204048	0.93249054
800	0.93160905	0.93161048	0.93204048	0.93249054

## VI. DISCUSSION

The whole experimental procedure rebels that by considering different techniques, such as DenseNet-121 with XG-Boost Classifier, and EfficientNetB0 technique with different depth range 3- 5, the estimator range from 100 to 800, we achieved different results, as shown in Table I to VI. Table I shows that the technique named DenseNet-121 with XG-Boost Classifier with depth 3 outreaches an accuracy of 0.94468524 in 450 Estimator. Similarly, by changing the depth to 4 with the same DenseNet-121 with XG-Boost Classifier, the accuracy reaches 0.94489594 in the 750 range of estimator. By using EfficientNetB0 with XG-Boost Classifier, we can have a comparison with the other techniques and find the differentiation of accuracies in different estimators' range with diverse depth values. The learning rate for all the techniques with different depths and estimators are numbered with values of 0.1, 0.3, 0.5, and 0.7. Fig. 5 depicts the accuracy of several pre-trained models as well as customized XG-Boost models that incorporate characteristics collected by method 1. The proposed technique is compared with various existing state of art techniques i.e. VGG16, VGG19, InceptionResNet-V2, InceptionV3, MobileNetV2, ResNet101V2, ResNet50V2, Xception, and hence the proposed technique was found to have the highest accuracy in finding the COVID infection. The modified XG-Boost model was trained using Algorithm 1 and EfficientNetB0 features, which explains its accuracy of 0.976, or 97.6% which explains its accuracy of 0.976, or 97.6%. This is the best result as compared to previously proposed algorithms given in [22] [23].

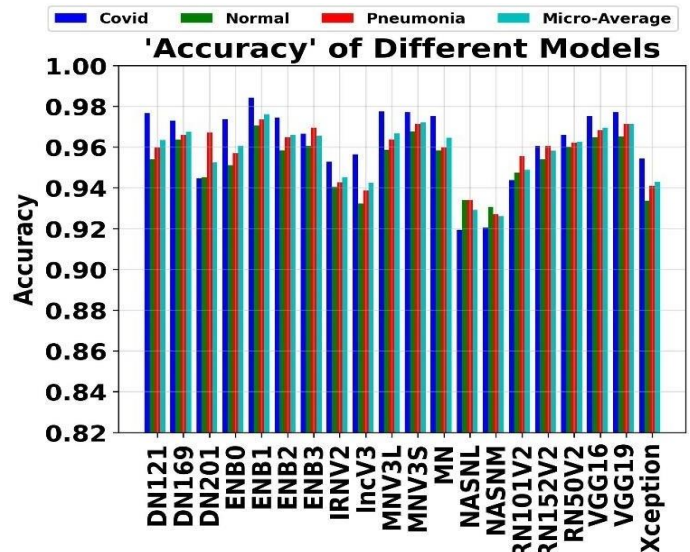


Fig. 5. Accuracy of tuned XGBoost models trained using deep features detection technique and various pre-trained models.

## VII. CONCLUSION

A Deep Feature Detection based method for identifying pneumonia and the COVID-19 virus in patients is

demonstrated using chest X-rays. After lung area segmentation, this article describes a two-stage method for extracting deep features from X-Ray images. These characteristics are then used to train the XG-Boost classifiers to distinguish between pneumonia patients, healthy people, and people infected with COVID-19. When the results of 20 different pre-trained models are compared, it is clear that using EfficientNetB0 for deep feature detection results in the best detection accuracy, precision, recall, specificity, and F1-score. The following values correspond to these criteria: 97.6%, 0.964, 0.964, and 0.982. These findings support the proposed strategy's efficacy. The tables show that the proposed diagnostic testing model was better than the competitive models. The proposed testing model is a technological alternative to COVID-19 testing tools. A CNN method for COVID-19 can be used to test image classification with a large dataset and complete with symptoms.

#### REFERENCES

- [1] Ravi, V., Narasimhan, H., Chakraborty, C. and Pham, T.D, "Deep learning-based meta-classifier approach for COVID-19 classification using CT scan and chest X-ray images", *Multimedia systems*, 28(4), pp.1401-1415, 2022.
- [2] Aggarwal, P., Mishra, N.K., Fatimah, B., Singh, P., Gupta, A. and Joshi, S.D., "COVID-19 image classification using deep learning: Advances, challenges, and opportunities", *Computers in Biology and Medicine*, p.105350, 2022.
- [3] Das, A., "Adaptive UNet-based Lung Segmentation and Ensemble Learning with CNN-based Deep Features for Automated COVID-19 Diagnosis", *Multimedia Tools and Applications*, 81(4), pp.5407-5441, 2022.
- [4] Trinh, Q. H., Nguyen, M. V., & Nguyen-Dinh, T. P. "Res-Dense Net for 3D Covid Chest CT-Scan Classification", In *International Conference on Image Analysis and Processing*, pp. 483-495, 2022.
- [5] Yildirim, M., Eroglu, O., Eroglu, Y., Çinar, A. and Cengil, E., "COVID-19 Detection on Chest X-ray Images with the Proposed Model Using Artificial Intelligence and Classifiers", *New Generation Computing*, pp.1-15, 2022.
- [6] Kaya, M. and Eris, M., "D3SENet: A hybrid deep feature extraction network for Covid-19 classification using chest X-ray images", *Biomedical Signal Processing and Control*, pp.104559, 2023.
- [7] Thamer, S.A. and Alshmmri, M.A., "Effective Diagnosing of Covid-19 from CXR Images Using Deep Learning Approaches and Optimized XG Boost Model", *JOURNAL OF ALGEBRAIC STATISTICS*, Vol.13, No.2, pp.1236-1250, 2022.
- [8] Pattanaik, P.A., Khan, M.Z. and Patnaik, P.K., "ILCAN: a new vision attention-based late blight disease localization and classification", *Arabian Journal for Science and Engineering*, Vol.47, No.2, pp.2305-2314, 2022.
- [9] Luz, E., Silva, P., Silva, R., Silva, L., Guimarães, J., Miozzo, G., Moreira, G. and Menotti, D., "Towards an effective and efficient deep learning model for COVID-19 pattern detection in X-ray images. Research on Biomedical Engineering, Vol. 38, No.1, pp.149-162, 2022.
- [10] Pattanaik, P.A., "Automated Segmentation for Knee Joint MRI Images Using Hybrid UNet+ Attention", In *2022 IEEE Trends in Electrical, Electronics, Computer Engineering Conference (TEECOCN)*, pp. 56-61, 2022.
- [11] Luz, E., Silva, P., Silva, R., Silva, L., Guimarães, J., Miozzo, G., Moreira, G. and Menotti, D., "Towards an effective and efficient deep learning model for COVID-19 patterns detection in X-ray images", *Research on Biomedical Engineering*, Vol. 38, No. 1, pp.149-162, 2022.
- [12] A. HaghaniFar, M. M. Majdabadi, Y. Choi, S. Deivalakshmi, and S. Ko, "COVID-CXNet: Detecting COVID-19 in frontal chest X-ray images using deep learning," *Multimed. Tools Appl.*, vol. 81, no. 21, pp. 30615–30645, Sep. 2022, doi: 10.1007/s11042-022- 12156-z.
- [13] M. Shorfuzzaman, M. Masud, H. Alhumyani, D. Anand, and A. Singh, "Artificial Neural Network-Based Deep Learning Model for COVID-19 Patient Detection Using X-Ray Chest Images," *J. Healthc. Eng.*, vol. 2021, 2021, doi: 10.1155/2021/5513679.
- [14] M. D. K. Hasan et al., "Deep Learning Approaches for Detecting Pneumonia in COVID-19 Patients by Analyzing Chest X-Ray Images," *Math. Probl. Eng.*, vol. 2021, 2021, doi: 10.1155/2021/9929274.
- [15] J. Li, D. Zhang, Q. Liu, R. Bu, and Q. Wei, "COVID-GATNet: A Deep Learning Framework for Screening of COVID-19 from Chest X-Ray Images," in *2020 IEEE 6th International Conference on Computer and Communications, ICC 2020, 2020*, pp. 1897–1902, doi: 10.1109/ICCC51575.2020.9345005.
- [16] D. Dansana et al., "Early diagnosis of COVID-19-affected patients based on X-ray and computed tomography images using deep learning algorithm," *Soft Comput.*, 2020, doi 10.1007/s00500-020-05275-y.
- [17] K. Hammoudi et al., "Deep Learning on Chest X-ray Images to Detect and Evaluate Pneumonia Cases in the Era of COVID-19," *J. Med. Syst.*, vol. 45, no. 7, 2021, doi: 10.1007/s10916-021-01745-4.
- [18] A. U. Ibrahim, M. Ozsoz, S. Serte, F. Al-Turjman, and P. S. Yakoi, "Pneumonia Classification Using Deep Learning from Chest X-ray Images During COVID-19," *Cognit. Comput.*, 2021, doi 10.1007/s12559-020-09787-5.
- [19] A. I. Khan, J. L. Shah, and M. M. Bhat, "CoroNet: A deep neural network for detection and diagnosis of COVID-19 from chest x-ray images," *Comput. Methods Programs Biomed.*, vol. 196, 2020, doi 10.1016/j.cmpb.2020.105581.
- [20] H. Panwar, P. K. Gupta, M. K. Siddiqui, R. Morales-Menendez, P. Bhardwaj, and V. Singh, "A deep learning and grad-CAM based color visualization approach for fast detection of COVID-19 cases using chest X-ray and CT-Scan images," *Chaos, Solitons and Fractals*, vol. 140, 2020, doi: 10.1016/j.chaos.2020.110190.
- [21] E. Luz et al., "Towards an effective and efficient deep learning model for COVID-19 patterns detection in X-ray images," *Res. Biomed. Eng.*, vol. 38, no. 1, pp. 149–162, Mar. 2022, doi: 10.1007/s42600-021-00151-6.
- [22] C. Zhang et al., "ResNet or DenseNet? Introducing dense shortcuts to ResNet," in *Proceedings - 2021 IEEE Winter Conference on Applications of Computer Vision, WACV 2021, 2021*, pp. 3549–3558, doi: 10.1109/WACV48630.2021.00359.
- [23] Luz, E., Silva, P., Silva, R., Silva, L., Guimarães, J., Miozzo, G., Moreira, G. and Menotti, D., "Towards an effective and efficient deep learning model for COVID-19 patterns detection in X-ray images", *Research on Biomedical Engineering*, Vol. 38, No.1, pp.149-162, 2022.
- [24] Lunagariya, M. and Katkar, V., "Light Weight Approach for COVID-19, Pneumonia Detection from X-Ray Images using Deep Feature Extraction and XGBoost", In *2022 Second International Conference on Computer Science, Engineering and Applications (ICCSEA)*, pp. 1-5, 2022.